J Physiol 589.10 (2011) pp 2515–2528

The Journal of Physiology

Neural mechanism of activity spread in the cat motor cortex and its relation to the intrinsic connectivity

Charles Capaday[1], Carl van Vreeswijk[2], Christian Ethier[3], Jesper Ferkinghoff-Borg[1] and Doug Weber[4]

[1]*Brain and Movement Laboratory, Department of Electrical Engineering, Section of Biomedical Engineering, Danish Technical University, Lyngby, Denmark*
[2]*Neurophysique et Physiologie du Système Moteur, CNRS UMR 8119, Paris, France*
[3]*Department of Physiology, Faculty of Medicine, Northwestern Univeristy, Chicago, IL, USA*
[4]*Department of Physical Medicine & Rehabilitation and Department of Bioengineering, University of Pittsburgh, Pittsburgh, PA 15213, USA*

Non technical summary The motor cortex (MCx) is an important brain region that initiates and controls voluntary movements. Neurons in MCx are anatomically connected by recurrent (feedback) networks. This connectivity pattern allows neurons to communicate reciprocally with each other potentially over distances of 6–7 mm. However, how far such neural activity is actually communicated was not known. We found that the activity of a small cortical point, about 0.4 mm in radius, activates a surrounding territory of approximately 7.22 mm^2 in area. This is smaller than the area covered by the anatomical connections, indicating the existence of mechanisms that limit the spread of activity. Nonetheless, such an area contains the representations of a variety of muscles spanning several joints, from digits to shoulder. These results support the hypothesis that the MCx controls the forelimb musculature in small synergistic groups, rather than singly and separately. Understanding motor cortical physiology is important for the design of neuro-prosthesis to interface the brain to paralysed muscles.

Abstract Motor cortical points are linked by intrinsic horizontal connections having a recurrent network topology. However, it is not known whether neural activity can propagate over the area covered by these intrinsic connections and whether there are spatial anisotropies of synaptic strength, as opposed to synaptic density. Moreover, the mechanisms by which activity spreads have yet to be determined. To address these issues, an 8 × 8 microelectrode array was inserted in the forelimb area of the cat motor cortex (MCx). The centre of the array had a laser etched hole ∼500 μm in diameter. A microiontophoretic pipette, with a tip diameter of 2–3 μm, containing bicuculline methiodide (BIC) was inserted in the hole and driven to a depth of 1200–1400 μm from the cortical surface. BIC was ejected for ∼2 min from the tip of the micropipette with positive direct current ranging between 20 and 40 nA in different experiments. This produced spontaneous nearly periodic bursts (0.2–1.0 Hz) of multi-unit activity in a radius of about 400 μm from the tip of the micropipette. The bursts of neural activity spread at a velocity of 0.11–0.24 m s^{-1} (mean = 0.14 mm ms^{-1}, SD = 0.05) with decreasing amplitude. The area activated was on average 7.22 mm^2 (SD = 0.91 mm^2), or ∼92% of the area covered by the recording array. The mode of propagation was determined to occur by progressive recruitment of cortical territory, driven by a central locus of activity of some 400 μm in radius. Thus, activity did not propagate as a wave. Transection of the connections between the thalamus and MCx did not significantly alter the propagation velocity or the size of the recruited area, demonstrating that the bursts spread along the routes of intrinsic cortical connectivity. These experiments demonstrate that neural activity initiated within a small motor cortical locus (≤400 μm in radius) can recruit a relatively large neighbourhood in which a variety of muscles acting at several forelimb joints are represented.

DOI: 10.1113/jphysiol.2011.206938

These results support the hypothesis that the MCx controls the forelimb musculature in an integrated and anticipatory manner based on a recurrent network topology.

(Resubmitted 4 February 2011; accepted after revision 21 March 2011; first published online 21 March 2011)
Corresponding author C. Capaday: Brain and Movement Laboratory, Department of Electrical Engineering, Section of Biomedical Engineering, Danish Technical University, Ørsteds Plads, Building 349, 2800 Kgs. Lyngby, Denmark. Email: charles.capaday@ccapcable.com

Abbreviations BIC, bicuculline; EMG, electromyographic; MCx, motor cortex; MUA, multi unit activity; PCA, principal component analysis; RMS, root mean square.

Introduction

The operational principles, neural circuitry and indeed the very functions subserved by the motor cortex (MCx) continue to be unravelled (e.g. Graziano *et al.* 2002; Capaday, 2004; Weiler *et al.* 2008; Capaday *et al.* 2009). For example, cortical points are linked by a recurrent neural network topology (Capaday *et al.* 2009) and the inputs from layers II/III to layer V are amplified (Weiler *et al.* 2008). Individual muscles are represented in multiple non-contiguous cortical loci in combination with a variety of other muscles acting at the same or different joint(s) (e.g. Donoghue *et al.* 1992; Schneider *et al.* 2001; Sanes & Schieber, 2001). Movement related muscle synergies may be recruited by selective excitation and simultaneous disinhibition of cortical points (Schneider *et al.* 2002). Moreover, the evoked electromyographic (EMG) outputs of separate motor cortical points sum linearly, an operational principle that may facilitate the synthesis of motor commands (Ethier *et al.* 2006). This neurophysiological finding lends support to the hypothesis that movement related EMG activities are synthesized by the linear combination of a small number of basic muscle synergies (d'Avella *et al.* 2006).

We recently showed that motor cortical points are linked by intrinsic horizontal connections according to a recurrent neural network topology (Capaday *et al.* 2009). The connection strength, as determined by the synaptic boutons density, decreases monotonically as a function of the radial distance between points. However, the details and functional significance of the connectivity pattern remain to be elucidated. In particular it is not known whether neural activity can propagate over the area covered by the intrinsic connections, or whether there are spatial anisotropies of synaptic strength, as opposed to synaptic density. Moreover, the mechanisms by which neural activity spreads have yet to be determined. Data obtained in cortical slice preparations and mathematical models developed from these suggest that propagation of neural activity is wave-like, but this has not been demonstrated *in vivo*, where the connectivity is intact (Chagnac-Amitai & Connors, 1989; Golomb & Ermentrout, 1999). Consequently, the purpose of this study was threefold. First, to determine whether neural activity can propagate along the routes of intracortical connectivity we recently demonstrated. Second, to determine whether there are anisotropies of effective synaptic strength and propagation velocity which may not be deduced from the anatomical connectivity. Lastly, we sought to elucidate the mode of activity propagation *in vivo*.

To address these issues, experiments were performed in the forelimb area of the cat MCx. Focal bursts of neural activity were induced by iontophoretic application of the $GABA_A$ receptor antagonist bicuculline methochloride (BIC). The spread of this activity was measured from multi-unit activity (MUA) recordings made by an 8×8 array of silicon microelectrodes. The sparse nature of the connectivity between individual cortical neurons makes it difficult to address the issue of cortical activity propagation with single unit recordings. By contrast, connections between small groups of neurons are more likely. Furthermore, activity in such neuron populations would be readily evoked by synchronized high rate inputs, such as those produced by discharges of an ictal cortical focus. Focal ictal discharges are induced by the local application of epileptogenic substances such as penicillin and bicuculline (Ajmone-Marsan, 1969; Prince & Wilder, 1967). The resulting ictal focus produces recurrent bursts of high-rate neural activity (Capaday, 2004). We thus reasoned that recording the activity of local neuron populations at different cortical sites in response to a synchronized input should provide answers to the posed questions. By contrast to single unit recordings, MUA recordings are easy, do not require single unit identification procedures and are very stable over time (Stark & Abeles, 2007). MUA recordings represent the weighted average of single spike activity recorded within some 100 μm from the microelectrode tip (Buchwald *et al.* 1965; Buchwald & Grover, 1970; Legatt *et al.* 1980). Importantly for the present study, MUA recordings obtained from multiple cortical sites, when taken together, yielded more accurate predictions of movement parameters than any other intracortical signal (Stark & Abeles, 2007).

A summary of this work was published as an abstract (Capaday *et al.* 2006).

Methods

The data reported here were obtained from nine male cats weighing between 3.0 and 4.5 kg. The study was approved by the local ethics committee and conformed to the procedures outlined in the *Guide for the Care and Use of Laboratory Animals*, published by the Canadian Council for Animal Protection.

Experimental rationale

A practical experimental outcome of our recent body of work on the cat MCx was the development of a relatively simple neurochemical method to activate the motor cortical circuitry (e.g. Schneider *et al.* 2002; Ethier *et al.* 2006; Capaday, 2004). Microiontophoretic ejection of BIC induces bursts of neural activity that recur nearly periodically (Fig. 1*A*). BIC is likely to exert its action by disinhibition, biasing the neural circuitry to a highly excitable state. In this way, a randomly occurring excitatory input leads to a highly amplified output composed of the synchronized discharge of a large number of neurons located within a radius of 250–400 μm from the micropipette tip (e.g. Tremere *et al.* 2001; Schneider *et al.* 2002). BIC does not affect fibres of passage and the evoked spikes are conducted orthodromically. There are two important points concerning these BIC induced bursts of activity. First, they are of neural origin and therefore do not interfere with electrical recordings as does microstimulation. Secondly, when the bursts reach sufficient amplitude they evoke electromyographic (EMG) activity and coordinated limb movements (Capaday, 2004; Ethier *et al.* 2006). Of course BIC does not activate the neural circuitry as occurs during normal brain activity. Nonetheless, we have shown that the pattern of muscle activity evoked by the BIC induced cortical bursts is nearly identical to that evoked by microstimulation of the same cortical point (Ethier *et al.* 2006; Capaday *et al.* unpublished observations). Similarly, Cooke & Graziano (2004) have demonstrated that defensive movements represented in a polysensory area of the monkey motor cortex can be released by an air puff to the face, or by objects approaching the face, following application of BIC in that zone. Importantly, the same reaction is obtained by microstimulation of this cortical area (Cooke & Graziano, 2004). Taken together, these results demonstrate that BIC-induced bursts of neuronal activity evoke the natural output of the affected area, and this is a useful method to investigate cortical physiology. In this study we asked whether the activity of such an endogenous 'neural signal generator' is propagated to other parts of the MCx along the routes of intrinsic connectivity. We also measured the size of the cortical area recruited (activated) by the endogenous burst and the propagation velocity, and determined the mechanism by which activity propagates.

Animal preparation

Details on surgical procedures, electrophysiological methods and homeostatic measures used in the present study can be found in previous reports from this laboratory (e.g. Capaday *et al.* 1998; Schneider *et al.* 2001, 2002; Capaday *et al.* 2009). Briefly, the animals were anaesthetized with an intramuscular injection of ketamine (33 mg kg^{-1}) and xylazine (1 mg kg^{-1}). Once the surgical procedures terminated, a perfusion pump was connected to a cannula in the femoral vein and a steady flow of anaesthetic (10–30 mg h^{-1} ketamine, depending on the animal) was delivered throughout the experiment. The blood pressure (BP) was recorded from the femoral artery. The anaesthetic level was adjusted to (1) keep the BP near 100 mmHg, which in our long experience seems the simplest and most direct physiological variable to assess the level of anaesthesia and (2) not to have a withdrawal reflex upon pinching the paw, the two criteria being associated. The femoral vein cannula also served to deliver 5 ml of glucose solution every 2 h. The animal's temperature was kept near 37°C by a heating blanket wrapped around the animal's trunk and by an overhead heat lamp. In two animals connections between the MCx and thalamus were severed using a blunted surgical needle undercutting the cortex to create a cortical island.

Iontophoresis

Local GABAergic synaptic transmission was reduced at a cortical point by iontophoretic ejection of the $GABA_A$ antagonist bicuculline methiodide (Schneider *et al.* 2002; Capaday & Rasmusson, 2003). The drug was dissolved at a concentration of 10 mM in distilled water and ejected from micropipettes having tip diameters of about 2–3 μm with positive currents of 20–40 nA for about 2 min. Gabazine is also a specific $GABA_A$ receptor antagonist, whereas bicuculline (BIC) may also block Ca^{2+} activated K^+ channels (Seutin & Johnson, 1999). The results obtained in previous experiments with either drug were similar (Ethier *et al.* 2006). However, BIC effects proved to be reversible after about 1 h, whereas those of Gabazine were more protracted.

Implanting the multi-unit arrays

The 8 × 8 silicon microelectrode arrays (Utah arrays) used in these experiments were manufactured by Blackrock Systems (Salt Lake City, UT, USA). The length of the microelectrodes was 1500 μm and the distance between their tips was 400 μm. A hole about 500 μm in diameter was laser etched in approximately the middle of the array (Fig. 1*B*, inset). This allowed the insertion of the tip of a fine glass micropipette into the underlying cortex at a depth of about 1200 μm. The array was inserted through

a large craniotomy into the coronal gyrus, usually anterior to the cruciate sulcus. This area of the cat MCx contains a significant portion of the forelimb representation. To easily handle the array for implantation we used a 2.9 mm (OD) stainless steel (s.s.) tube attached to a vacuum, with a pressure control valve in between the vacuum and the s.s. tube. The array was gently maintained in place on the surface of the cortex while the wire bundle was tacked down to the skull with bees' wax. Before positioning the pneumatic inserter over the array for implantation, the array was briskly pushed down manually through the pia using the s.s. tube. With the wire bundle tacked down and the array secured onto the pia, the head of pneumatic inserter was positioned parallel to the bond surface of the array. A single pressure pulse applied to the piston of the inserter drove the array into the cortex at high velocity to a depth of about 1500 μm. Single unit activity always appeared within minutes on several electrodes of the array and within 20–30 min activity was recorded on more than half of the electrodes. Photographs of the array and procedural details are available at the laboratory's web site (http://www.brainandmovementlab.org/).

Signal processing, data reduction and quantitative analysis

Microelectrode signals (Fig. 1*A*) were high pass filtered at 300 Hz, low pass filtered at 5 kHz and sampled at 10 kHz in real-time by a Cerebus-128 recording system. Records of 5 min duration were obtained before ejection of BIC and during the ejection, which typically lasted for 5 min, and several more recordings were made thereafter during the protracted period of spontaneous bursting. The signals were stored on a computer disk for off-line data reduction and analysis. All data reduction, signal processing and analysis procedures were done by custom programs written in MATLAB (The Mathworks, Inc., Natick, MA, USA). Microelectrode signal values were squared and smoothed using a 1.6 ms time constant, and the root mean square (RMS) value calculated in steps of 1 ms. These operations are closely related to the simple combination of rectification and low-pass exponential filtering and have a long tradition in the analysis of EMG signals. From visual inspection of the recording channel having the largest bursts, a threshold value at least 3 standard deviations (SD) above the noise level was determined. This served as a time reference value around which to trigger the averaging of 8–16 consecutive bursts in each channel. Thus, the average burst response at each electrode was derived from continuous records (Fig. 1*B*). Typically, the averaging was done over a time span of 100 ms before and 300 ms after the trigger marker, making for an averaging window of 400 ms duration. The DC value of the background activity in each average record was estimated over a 50–100 ms time window preceding the burst and subtracted from the average. To visualize the locus of burst initiation and its spatial spread, activity maps were constructed as follows. The RMS value in each average record was measured at time increments of 1 ms, from the beginning to the end of the record. For each time step, this resulted in a 64×1 data vector which was mapped as an 8×8 data matrix, preserving the spatial relationship of the electrodes in the array. Thus, each entry in an 8×8 data matrix represents the level of activity at a single electrode of the array, at a given time. These representations of the data will be referred to as activity maps. Note that the laser etching removed the recording electrode near the centre of the array. For cosmetic display purposes, an entry at the appropriate location in the activity maps, consisting of the mean activity at the four electrodes adjacent to the hole, was made.

From the activity maps the spatial position of the barycentre of neural activity (commonly termed 'centre of gravity'), the size of the cortical area recruited and the inter-channel correlation matrix were determined. Specifically, to determine whether activity propagated to any given electrode, the activity level had to exceed 3 SD above the mean background activity at that electrode. Visual inspection of a multitude of records confirmed the validity of our automated algorithm. The cortical area activated could thus be determined from the fraction of activated electrodes relative to the total number, multiplied by the surface area of the recording array. Propagation velocity was determined from the inter-channel cross-correlation functions. A reference channel having the earliest burst onset time near the site of BIC ejection was selected. This was usually also the channel having the largest burst. Cross-correlation functions were calculated between this and all other channels, resulting in one auto-correlation and 63 cross-correlation estimates. The time lag at which peak correlation (optimal lag) occurred was determined from each of these lagged correlation estimates. The distance between the reference electrode and all other electrodes in the array was calculated and plotted against the corresponding optimal time lags. The best fitting least-means-squares line was determined. The slope of this line gives an estimate of propagation velocity. It should be noted that if the reference channel is incorrectly selected, the correlation between distance and optimal time lag is poor. Typically only one or two adjacent reference channels near the centre of the array resulted in a statistically significant correlation between these variables. This demonstrates that activity was initiated at a small cortical focus of about 400 μm in radius. Furthermore, estimates of propagation velocity were obtained from repetitions of this experiment in the same animal and the results always proved to be consistent.

A principal component analysis (PCA) based on eigenvalue decomposition of the data covariance matrix was also performed. The PCA was performed on the data matrix of average records as well as on continuous records of 20–30 s duration.

Results

The results are presented in three parts. First we report the results of experiments to determine how far neural activity initiated at a cortical locus spreads and the velocity at which it propagates. Second, we present results suggesting a non-wavelike mechanism of activity propagation. In the final section, we present evidence that the propagation of neural activity in our experiments did not significantly depend on cortico-thalamic feedback.

Characteristics of the multi-unit activity bursts

Iontophoretic ejection of BIC at a cortical point induces spontaneous nearly periodic bursts of multi-unit activity (MUA). The bursts are composed of high frequency synchronized discharges of multiple neurons (Fig. 1*A*). Note also the decreasing size of the MUA bursts with distance from the source of spontaneous activity. Inter-burst intervals depended on time since the start of BIC ejection, decreasing as time progresses. Typically, bursting starts at *ca* 0.2 Hz and may increase to near 1 Hz. The burst duration varied in different experiments between about 50 and 300 ms, typically increasing as ejection time progresses. The peak firing rate of single unit spikes within the burst, when these could be identified, ranged between 150 and 200 imp s^{-1}, the average firing rate being typically between 70 and 100 imp s^{-1}. These firing rates are within the known physiological range of cat MCx layer V neurons (Stafstrom *et al.* 1984). Continued ejection for approximately 2 min produces robust bursting that continues for some 40–60 min after removal of the micro-pipette. This allowed us to determine how far a burst of focal neural activity spreads and at what velocity. Examples of RMS-smoothed MUA bursts recorded at the source of spontaneous activity and at 1200 and 2000 μm are shown in Fig. 1*B*. The MUA signals processed in this way will be referred to as population responses, or population spikes. Typically, at or near the source, the population spike has a prominent phasic component followed by a longer lasting tonic component of much lower amplitude (Fig. 1*B*). The population spike recorded by electrodes further away (2000 μm) has an essentially phasic character (Fig. 1*B*). In nearly all cases ($n = 32$ separate trials in nine animals) activity was initiated at one to three loci (electrodes) near the point of ejection. This will be referred to as the locus of spontaneous activity initiation, or simply as the locus of initiation.

Typical results of a PCA of the data matrix representing the RMS-smoothed MUA bursts are shown in Fig. 2. The first principal component usually accounted for >80% of the total data variance, with the second principal component accounting for an additional 5–11% (Fig. 2*A*). In all cases, the waveform of the data projected on the first principal component (pc1) closely resembled the mean burst calculated across all recording channels (Fig. 2*B*). That of the data projected on the second principal component (pc2) was very nearly the first time derivative of the former (Fig. 2*B*). Two principal conclusions derive from these observations. First, most of the total power, as measured by the RMS value, is contained in only a few

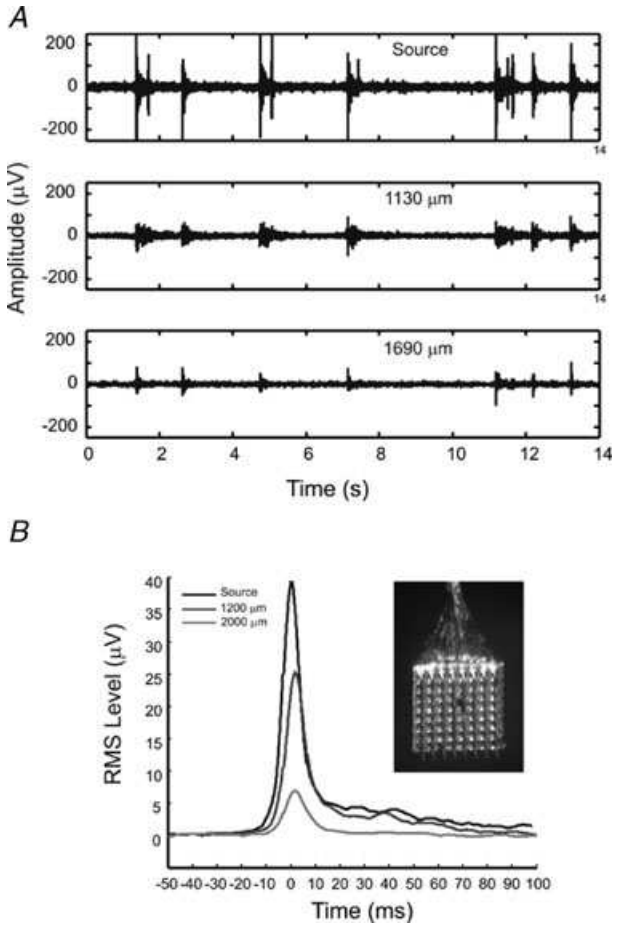

Figure 1. Examples of raw and RMS-smoothed MUA bursts
A, example of multiunit bursts recorded at three microelectrodes of the array. Note the recurrent and nearly periodic nature of the bursts. The distance of the electrodes from the locus of initiation (source) is given in the inset of each graph. *B*, examples of RMS-smoothed multi-unit bursts recorded at a distance of 1200 and 2000 μm from the source of BIC ejection. Time zero in this plot is relative to the peak of activity at the source. Note the decreased waveform amplitude and time lag with distance and that the tracings in *A* and *B* are from different recordings. A photograph of the array is shown as an inset in *B*; note the hole near the centre of the array. The electrode array covers an area of 2.8 × 2.8 mm^2.

recording channels. Second, the signals in the different recording channels are strongly linearly related to each other, differing mainly in amplitude and time to peak. Thus, the signals can be reconstructed with high fidelity by weighting a basic shape (pc1) and its first time derivative (pc2). These characteristics have important implications as to the mechanism of activity spread and justify using the cross-correlation function to estimate the spatial velocity of neural activity propagation.

Spatial activity spread and propagation velocity

MUA bursts at the locus of initiation spread, in all cases, across a wide expanse of the motor cortex covered by the recoding array (Fig. 3). The amplitude of the population response at each electrode was calculated every millisecond and displayed in activity maps, as shown in Fig. 3. The activity maps show the amplitude of the population response at each electrode of the recording array at the corresponding time step. In the example shown in Fig. 3, activity is initiated near the point of BIC ejection at coordinates (6, 5) of the array. The coordinates of the hole through which the iontophoretic micropipette was inserted was at coordinates (5, 5) in all recording arrays. Note the progressive recruitment of activated cortical territory with time. Activity was evoked at 62/64 recording electrodes in the example shown in Fig. 2. The recruited (activated) cortical area was 7.6 mm^2, or 96% of the cortical area covered by the array. Importantly, note also that at the time of maximal spatial recruitment, activity at the locus of initiation is high and in fact at or near its maximum. In a total of $n = 32$ repetitions of this experiment in nine animals, the area activated was on average 7.22 mm^2 (SD = 0.91 mm^2), or ~92% of the area covered by the recording array.

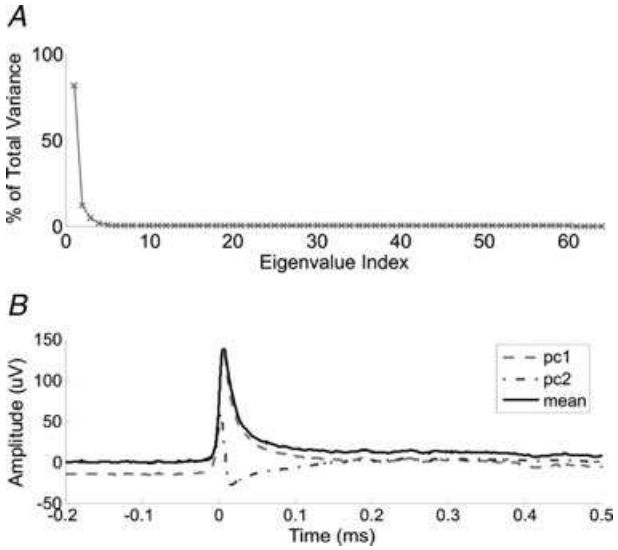

Figure 2. An example of typical results obtained from a PCA of the multiunit bursts
A, the first two principal components account for 93% of the total data variance as determined by the eigenvalues sorted in non-increasing order. *B*, the data projected onto the first two principal components (eigenvectors). The waveform of the data projected onto the first principal component (pc1) is closely related to the mean burst calculated across all recording channels. The waveform of the data projected onto the second principal component (pc2) is very nearly the first derivative of pc1. Note that because pc1 is normalized in amplitude to the peak of the mean burst it has a different DC offset.

The velocity at which activity propagated across the cortex was determined from cross-correlation functions as described in the methods. Two examples of propagation velocity estimates obtained from different animals are shown in Fig. 4. A linear relation between distance and latency is apparent, despite the scatter of data points. In the examples shown, the linear model accounts for, respectively, 73% and 79% of the data variance (r^2). In fact a linear model accounted best for the data variance in comparison to a quadratic relation. The best correlation between distance and latency depended critically, in all cases, on the choice of the reference electrode/channel for the cross-correlation estimates of latency. In the example shown in Fig. 4, electrode/channel 36 was the reference. But, if the adjacent electrode/channel 44 was used to obtain the cross-correlation estimates of latency, the r^2 value decreased from 0.74 to 0.44. The mean propagation velocity estimated from data obtained in 10 animals was 0.14 mm ms^{-1} (SD = 0.05; range, 0.11–0.24 mm ms^{-1}). Two other methods were also used to estimate propagation velocity, as explained in the methods. One method involved dividing the square-root of the maximally activated area by the time taken to reach this maximum. The time to peak of the population activity at each electrode was also used to estimate propagation velocity. Both measures gave results similar to those obtained by the cross-correlation method. The estimates based on time to peak measures yielded, however, lower correlation coefficients than those obtained by the cross-correlation measure. Note that in the graphs shown in Fig. 4 there is an obvious y-intercept. That is the best fit least-mean-squares line does not regress to the origin. The typical estimates of the y-intercepts were in the range between 400 and 500 μm. There are at least three explanations for this consistent observation. First, there is a minimal distance of 400 μm between the tips of the microelectrodes in the recording array. The discrete nature of the distance measures will result in a non-zero y-intercept, simply because the tip of the micropipette may not be immediately adjacent to any of the electrodes. Second, diffusion of BIC from the tip of the micropipette makes the locus of initiation of finite size (i.e. not a point source). This is manifest by activity occurring simultaneously at sometimes more than one electrode near the point of BIC ejection. Lastly, a simple model of

activity propagation predicts a non-zero *y*-intercept due to synaptic delay and synaptic integration time. These issues will be dealt with in detail in the Discussion.

On the nature of activity spread

A plot of the amplitude of the population response at each electrode of the array *vs.* its 2D Cartesian coordinates is shown in Fig. 5*A*. The surface plot shown corresponds to the time of maximum spatial recruitment. It can be observed that activity at the locus of initiation is higher than elsewhere. The barycentre of neural activity of the maps shown in Fig. 3, calculated every millisecond, is shown in Fig. 5*B*. The barycentre remains near the point of burst initiation, throughout the period of activity, as cortical territory is recruited and derecruited. This observation shows that activity spreads in an approximately radially symmetrical manner and is consistent with the idea that the progressive recruitment of cortical territory depends on sustained activity at the locus of initiation. The activated cortical area increased as an approximately sigmoidal function of time (Fig. 6). More importantly, the time at which the plateau was reached corresponded closely to the time at which activity at the locus of initiation peaked (Fig. 6*A* and *B*). Taken together, these observations suggest that neural activity did not propagate as a travelling wave; this point will be dealt with in detail in the Discussion.

Activity spread depends on intracortical connectivity

Connections between the motor cortex and thalamus were severed in two animals. Sensory activity could no longer

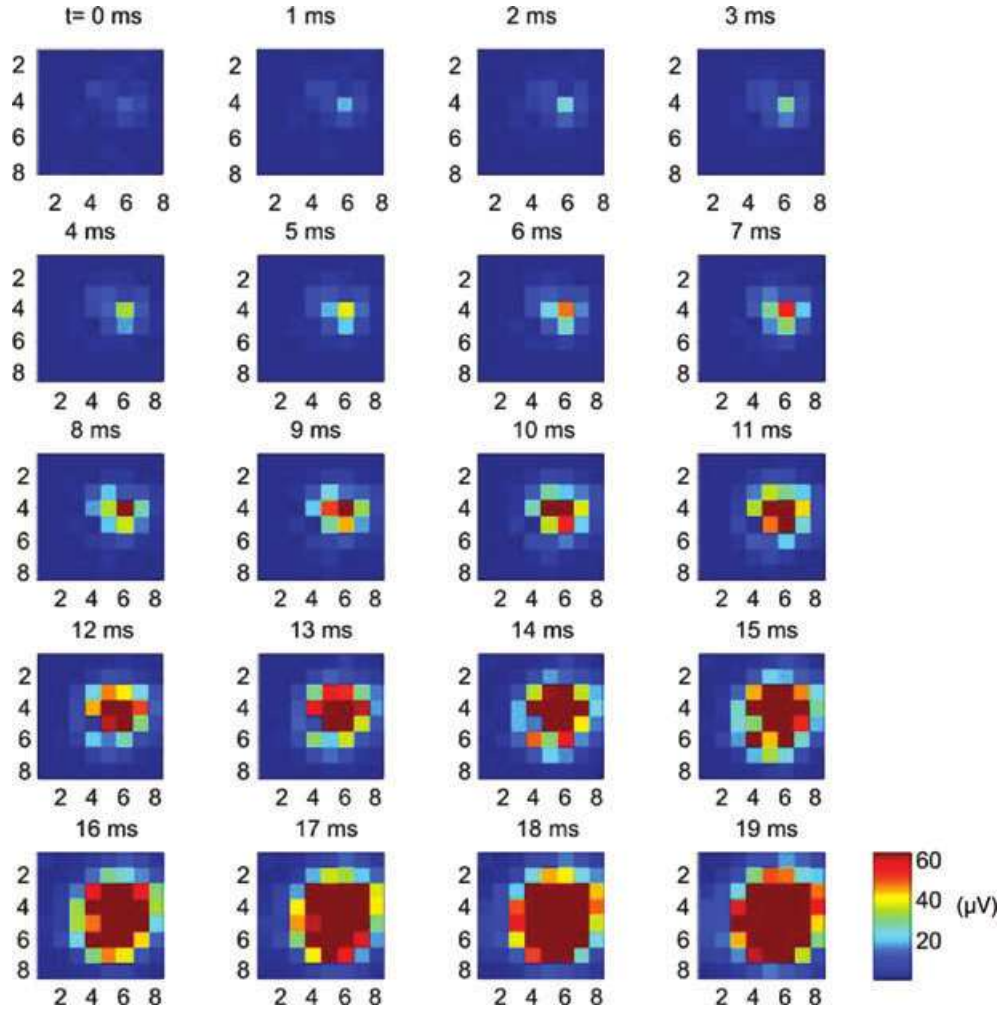

Figure 3. Example of activity maps calculated every millisecond from near the onset ($t = 0$ ms) of the spontaneous BIC-induced burst of neural activity to the time at which the maximum cortical area was recruited ($t = 19$ ms)
Activity continues for several tens of millisecond after that. Note the onset of activity at coordinate (4, 6) and the subsequent progressive recruitment of cortical territory with time. In this example activity was evoked at 62 out of 64 possible electrodes. The recruited cortical area was 7.6 mm^2, or 96% of the area covered by the array.

be evoked by, for example, tapping the dorsum of the paw. Before the lesion BIC was ejected for 5 min and data obtained to determine the spatial spread of activity and propagation velocity, as previously described. Note that in the intact brain repeating a BIC ejection some 2 h after the bursting produced by a first ejection has long subsided yields results qualitatively similar to those obtained after the first ejection. This demonstrates that no obvious residual effects remain by that time. Consequently, the lesions were made, in each case, 2 h after the initial BIC ejection. The level of spontaneous spike activity increased after the lesion. We waited about an hour post-lesion for this increased activity to subside before ejecting BIC anew. In this condition the spread of neural activity was similar to that in the intact brain. In the example shown in Fig. 7 the recruited cortical territory was 7.59 mm^2, or activity appearing at 62/64 electrodes, in the intact brain. After the lesion the recruited cortical territory was 7.47 mm^2, or activity appearing at 61/64 electrodes. The estimated propagation velocity was essentially the same before and after the lesion, respectively, 0.11 mm ms^{-1} and 0.10 mm ms^{-1}.

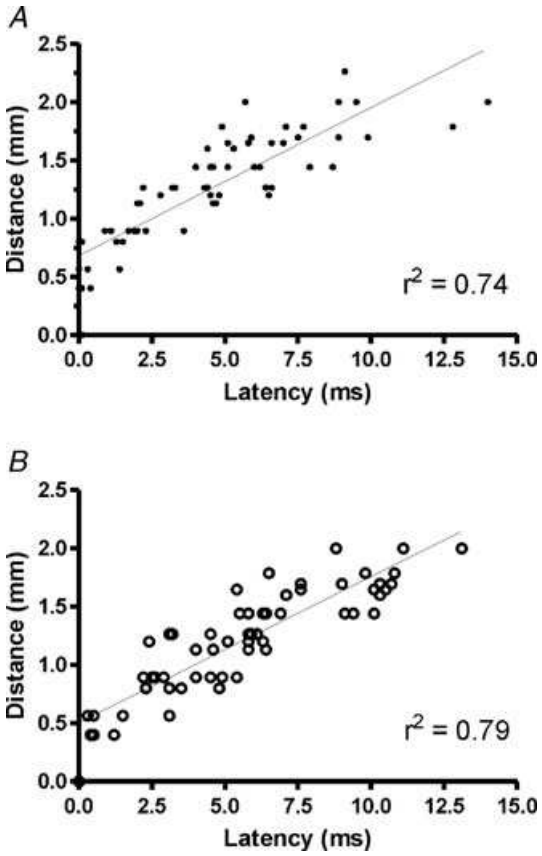

Figure 4. Examples of propagation velocity estimates based on cross-correlation measurements as described in the text
A and *B* are from different animals. The least-mean-square estimate of propagation velocity is 0.13 mm ms^{-1} in *A* and 0.12 mm ms^{-1} in *B*. The linear model accounts for 73% of the variance in *A* and 79% in *B*.

Discussion

Several observations on the propagation of neural activity in the MCx were reported. Iontophoretic ejection of BIC induced spontaneous recurring bursts of neural activity around the point of ejection. Therefrom, a cortical territory of about 6–7.8 mm^2 was recruited by neural activity spreading at a velocity of about 0.1–0.2 m s^{-1}. The peak firing rates near the point of BIC ejection were within the known physiological range as previously stated, but may exceed those observed in behaving animals (e.g. Lamarre *et al.* 1978; Cheney & Fetz, 1980). The spread

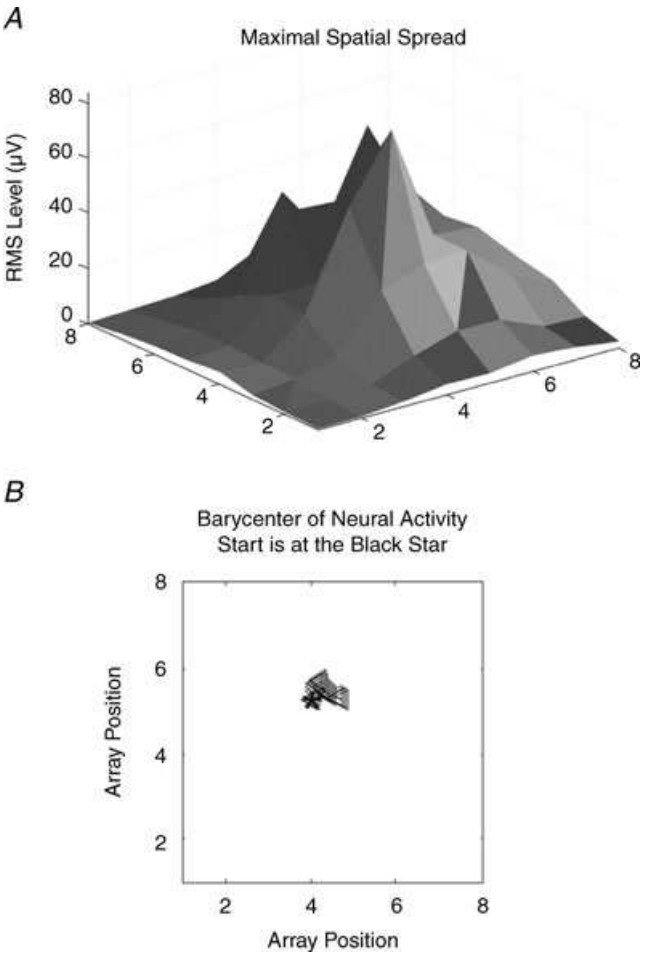

Figure 5. Plot of activity *vs.* array position at the time of peak activity at the source
The recruited cortical area reaches its maximum at the time activity at the source reaches its peak value. *A*, the barycentre of neural activity remains near the source of activity, at approximately coordinate (4, 6), as cortical territory is recruited and derecruited. *B*, the barycentre was calculated in steps of 1 ms, from burst initiation to burst termination. This is strong evidence that activity does not propagate as a travelling wave.

of activity depends on spatial and temporal summation, i.e. number of neurons discharging and their firing rates. Our measurements may be an upper limit, but usefully set the stage for future studies to determine the actual spread under natural conditions. Nonetheless, the areal spread we measured is consistent with the intrinsic connectivity pattern, as will be discussed further below. Interestingly, our estimates of spatial spread are smaller than those reported by other authors using different methods of recording and neural circuitry activation (e.g. Grinvald *et al.* 1994, Seidemann *et al.* 2002; Tolias *et al.* 2005). For example, the point spread function of a visual stimulus has a space constant of about 1.5×3 mm (Grinvald *et al.* 1994) in primary visual cortex (V1), as measured by optical imaging using voltage sensitive dyes (VSDs). The microstimulation evoked BOLD signal in V1 has a radial spread of some 5.8 mm (Tolias *et al.* 2005). We measured spiking activity, whereas the VSD and fMRI recording methods used in those studies are closely related to measures of synaptic activity (Grinvald *et al.* 1994; Logothetis, 2002). The large areal spreads obtained by VSD and fMRI measurements are likely to reflect subthreshold synaptic activity evoked at the distal ends of the long range horizontal connections. Our measurements of spiking activity may be more directly related to activation of the circuitry underlying overt movement production. The recruitment of cortical territory we measured did not depend on thalamocortical feedback connections and was thus essentially due to intrinsic horizontal cortical connections. We cannot totally discount the possibility of a thalamocortical contribution outside of the recording area; however this seems unlikely as activity at the edges of the array was always very low. Furthermore, in experiments where we injected at one of the edges of the array, activity typically did not invade the whole recording area. Consequently, the activated cortical area was well covered by our recording array. The time at which spatial recruitment of cortical territory reached its maximum closely corresponded to the time at which activity at the locus of initiation peaked. Importantly, the barycentre of neural activity remained at, or near, the locus of spontaneous burst initiation during recruitment and derecruitment of cortical territory.

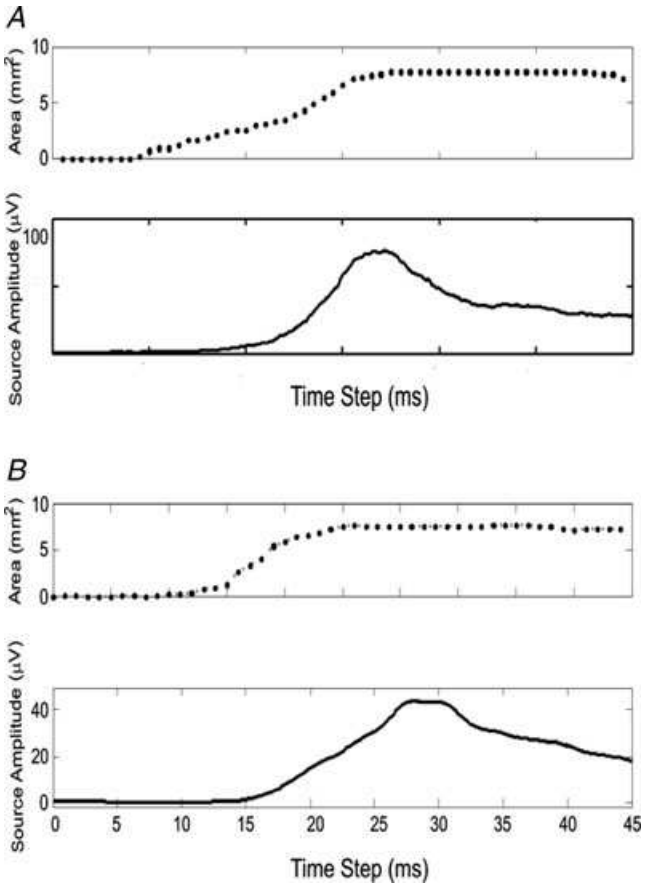

Figure 6. Two examples of the time course of MUA at the source of burst initiation (low pass filtered at 10 Hz) and the cumulative increase of recruited cortical territory
Note the close temporal coincidence between the time to peak activity at the source electrode and the time to recruitment plateau.

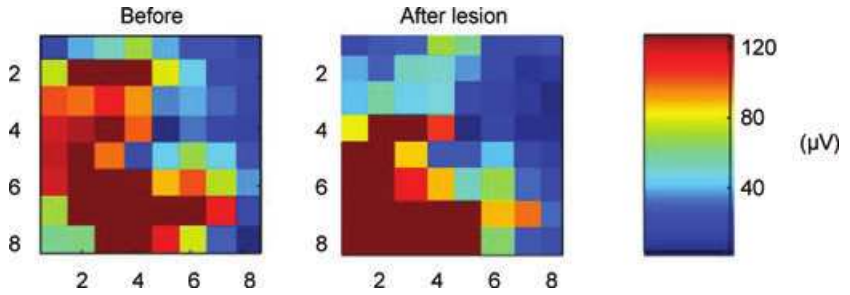

Figure 7. Following a lesion of the internal capsule linking the MCx to the thalamus, activity spread was similar to the intact brain condition
In this example the recruited cortical territory was 7.59 mm^2, or activity appearing at 62/64 electrodes, in the intact brain condition. After the lesion the recruited cortical territory was 7.47 mm^2, or activity appearing at 61/64 electrodes. The estimated propagation velocity was essentially the same before and after the lesion, respectively, 0.11 mm ms^{-1} and 0.10 mm ms^{-1}.

The possible mechanisms underlying these experimental findings and their significance will be discussed in turn. We will show that the estimated diffusion distance of BIC is consistent with a locus of spontaneous burst initiation having a radius of about 400 μm, which in part explains the non zero y-intercept of the distance *vs.* latency graphs. The idea that neural activity does not propagate as wave, but rather by progressive recruitment of cortical territory via long range horizontal connections, will be developed. We also make the point that the classical model of an excitatory centre and surround inhibition does not appear consistent with the spatial patterns of activity we have observed. The relatively large territory recruited by activity emanating from a relatively small locus contains a large variety of muscle representations. We will suggest that during normal physiological function, the horizontal spread of activities between cortical points constitutes feedforward sequencing control of the musculature. Related to this, the idea that a shifting focus of motor cortical activity can recruit a wide range of movement related EMG activities will be discussed.

The mean distance r travelled by a diffusing particle from the tip of a micropipette (i.e. a point source) is proportional to the square root of time. In a radially symmetrical situation in 3D, the mean diffusion distance is given by $r(t) = \frac{4}{\sqrt{\pi}}\sqrt{Dt}$, where D is the diffusion coefficient and t is time. In the restricted extracellular space of the cerebral cortex, however, D must be modified to take into account the tortuosity λ of the extracellular space; here we used $\lambda = 1.55$ (Nicholson & Phillips, 1981; Fox *et al.* 2003). The resulting, so called, apparent diffusion coefficient D^* is given by $D^* = D/\lambda^2$. The diffusion coefficient of BIC (MW $\approx$ 420) was estimated from the Setlow & Pollard (1962) charts to be about $D \approx 5 \times 10^{-6}$ cm^2 s^{-1} and thus $D^* \approx 2.1 \times 10^{-6}$ cm^2 s^{-1}. Given the protracted duration of the BIC evoked paroxysmal bursting, its uptake from the extracellular space can be, to a first approximation, ignored. From these considerations it can be calculated that the mean distance travelled by BIC molecules during 2 min of constant iontophoretic ejection was 360 μm. At distances greater than the average, the concentration drops off rapidly. For example, at $r = 360\,\mu$m the concentration is 45 μM, whereas at $r = 500\,\mu$m it is 7.6 μM, for a strong iontophoretic current of 40 nA and transport number of 0.2 (see Appendix 1). Thus, the locus of burst initiation should have a radius of $r \approx 400\,\mu$m. Given that the spacing between neighbouring electrodes is 400 μm, this estimate is consistent with the observation that simultaneous activity appeared at most at three electrodes adjacent to the point of BIC ejection. An area of some 400 μm in radius is well within the area of dense core horizontal connectivity identified in Capaday *et al.* (2009), measuring approximately 1.5 × 2.0 mm. It is likely, therefore, that the neurons within this locus will discharge nearly simultaneously because they are in a hyperexcitable state and strongly interconnected. We can conclude that the locus of BIC induced cortical bursting comprises an area some 400 μm in radius. This explains, in part, why the distance *vs.* latency graphs such as those shown in Fig. 4 have a non-zero y-intercept. The other contribution to the non-zero y-intercept is due to synaptic integration time, as developed below.

From the locus of burst initiation activity propagated at a velocity of 0.1–0.2 mm ms^{-1}, consistent with similar measurements made in primary visual cortex with voltage sensitive dyes (Grinvald *et al.* 1994). This propagation velocity may be a measure of the conduction velocity of thin unmyelinated intracortical axon collaterals as suggested by Grinvald *et al.* (1994), an explanation which we favour for the following reasons. The experimental latency values we measured are due to the sum of conduction time, synaptic transmission time and synaptic integration time (time to reach firing threshold). We can write this as $L_{exp} = L_{v_c} + L_{syn}$, where L_{exp} is the experimentally measured latency, L_{v_c} is the latency due to axonal conduction time and L_{syn} the sum of synaptic transmission and integration times. In Appendix 2 we derive a simple model relating latencies, conduction velocity (v_c) and the radius of the locus of initiation, d_0, to propagation distance, d. The equation thus obtained is:

$$d = L_{exp} v_c + (d_0 - L_{syn} v_c)$$

The terms in brackets being constants, the equation can be written as a simple linear relation $d = L_{exp} v_c + k$, where $k = (d_0 - L_{syn} v_c)$. Thus, according to this model the y-intercept of the distance *vs.* latency graphs is due to the size of the locus of initiation d_0 and synaptic factors L_{syn}. Importantly, the y-intercept does not affect the estimate of the slope of the relation, which is the propagation velocity. On these grounds, we favour the interpretation that our estimates of propagation velocity are, for the most part, estimates of the conduction velocity v_c of the fine axon collaterals that form the horizontal intracortical connections. As a final point on propagation velocity measures, spontaneous activity makes cortical points discharge somewhat out of sequence, explaining the variability of the data points in the distance *vs.* latency graphs.

Our fine scaled spatio-temporal measurements further our understanding of the mechanisms by which neural activity propagates within cortex. It has been thought that neural activity spreads in the cortex as a travelling wave, as in the model developed by Golomb & Ermentrout (1999). In this typical model, neural activity is transmitted serially from neuron to neuron. Once a neuron in the chain discharges, it is no longer active, its activation energy

being transferred to its nearest neighbour. The model is based on experimental results obtained in disinhibited cortical slices (Chagnac-Amitai & Connors, 1989). The nature of the activity spread observed in our experiments on the intact neocortex is not consistent with a wavelike mechanism of propagation. Our results demonstrate that propagation depends on sustained activity at the locus of initiation. Activity did not hop from locus to locus as is evident from the activity maps and the cumulative increase of recruited cortical area with time (Fig. 6). The barycentre of activity was always at, or near, the locus of initiation at the time that activity there reached its peak value. Importantly, this corresponded with the time to reach maximum recruitment of cortical territory (Fig. 5). These observations suggest that neural activity does not propagate as a travelling wave. Spatial propagation of activity depends on continued neural drive from the locus of initiation, a mechanism which is consistent with the extant long range horizontal fibres studded with synaptic boutons all along their course (Capaday *et al.* 2009). Moreover, the level of activity decreases with distance from the locus of initiation, reminiscent of the decrease of bouton density with distance from a cortical locus.

We suggest that the mode of propagation is as follows. Activity at the locus of initiation recruits neurons via the axon collaterals of the discharging neurons, which in turn recruit other neurons. Because the connections are recurrent, activity is fed back in the opposite direction. Axon terminals in the cortex, either from extrinsic or intrinsic sources, synapse onto every morphological or physiological neuronal type within their terminal projection field (White, 1989). Consequently, cortical neurons are activated by balanced excitatory and inhibitory currents (Haider *et al.* 2006; Okun & Lampl, 2008). This suggests that an excited central locus surrounded by an actively inhibited zone may not represent the activation profile within the MCx. Instead, we favour the explanation that propagation continues so long as excitatory currents exceed inhibitory currents sufficiently to discharge neurons. Two of the present observations support this suggestion. First, the monotonically decreasing nature of the bouton density and its parallel in the activity profiles (Fig. 5*A*). Second, the physiologically recruited cortical area is smaller than the area covered by the anatomical connections, but larger than the dense core of connectivity (Capaday *et al.* 2009). Also consistent with the non-patchy nature of the intrinsic motor cortical connectivity, clusters of activity were not observed, the bursts spread with monotonically decreasing amplitude. The essential reasons for the fall of signal amplitude as a function of radial distance are that (1) the number of recruited neurons and their population firing rate decrease with radial distance and (2) smaller units are recruited as a function of distance from the electrode, presumably following the size principle. This explanation is corroborated by examination of the raw MUA recording traces. Thus, the MUA recordings reflect the essential neurophysiological mechanisms involved in the spatial spread of neural activity.

Given a propagation velocity of 0.1–0.2 mm ms^{-1} (Capaday *et al.* 2006), an area of some 3 mm^2 (i.e. 1 mm in radius) would be activated in 5–10 ms. The pre-EMG activity of motor cortex neurons lasts tens of milliseconds (e.g. Cheney & Fetz, 1980; Lamarre *et al.* 1978). This would allow for extended spatial interactions prior to movement initiation and during the continued firing of the network. The results we have presented support the idea that communication between motor cortical neurons, at least in the cat MCx, occurs by an inclusive broadcast style of communication rather than by private lines (i.e. point to point). That is a cortical point controlling a given muscle(s) communicates its activity recurrently within a large neighbourhood in which a variety of muscles spanning several joints are represented (Capaday *et al.* 2009). Indeed in the present study, from observation of the BIC evoked movements it was clear that both proximal and distal muscles were recruited. Thus the area activated contained representations of muscles spanning the forelimb. The firing rate of neurons at any one cortical point thus reflects the state of the neighbourhood. What might be the functional consequences of this? The area recruited by a central locus of activity may correspond to that required to evoke coordinated forelimb movements. Indeed coordinated movements are elicited when BIC induced bursts reach sufficient amplitude and duration, as they do with long train microstimulation (Ethier *et al.* 2006). As already noted, the activated area encompasses representations of a wide variety of muscles reminiscent of the Jackson–Walshe perspective on motor cortical function (reviewed in Capaday, 2004). A basic tenet of their thesis is that activity at a cortical focus represents the leading part of a movement (e.g. paw) and that of parts further removed (e.g. wrist and elbow). Thus, the state of neural activity at any one cortical point in the recruited area and that of the area itself are anticipations of what additional muscles may need to be recruited as the movement evolves, or is perturbed. Sequencing, or anticipation, is a property of recurrent neural networks (Dayan & Abbott, 2001). Central to the Jackson–Walshe thesis is the idea of overlapping and graded movement representations as a mechanism underlying integrated control of the musculature. Indeed as surmised by those authors, our physiological measurements demonstrate that cortical points some 2.8 mm apart, or more, share considerable territory. Thus, cortical points are not functionally independent, they cannot operate in isolation. Finally, overlapping and graded movement representations allow for movement commands to be synthesized by the linear summation of outputs (Ethier

et al. 2006), as the focus of neural activity moves within the MCx.

Appendix 1. Diffusion from the tip of a micropipette

Methods for estimating the concentration of an iontophoretically ejected substance as a function of distance from the tip of the micropipette and time were developed by Nicholson and colleagues (e.g. Nicholson & Phillips, 1981; Nicholson & Sykova, 1998). The methods involved theoretical analysis based on the classic equations of diffusion and experimental measurements. Importantly, the analysis was grounded on the concept of apparent diffusion coefficient D^* introduced in the discussion, as well as that of volume fraction α. The latter is simply the ratio of the extracellular space available to diffusing particles to total volume of the diffusion medium. The flux Q of ions (source strength) ejected from the tip of a micropipette, in mol s^{-1}, is given by

$$Q = nI/F \tag{A1}$$

where n is the transport number which gives the proportion of the total current carried by the pharmacologically active ions, I is the iontophoretic current in amperes and F is Faraday's constant in C mol^{-1}. Values for n vary widely for different micropipettes and pharmacological agents, but are typically between 0.2 and 0.4. Using spherical polar coordinates with radial coordinate r, the solution to the diffusion equation for a point source (i.e. tip of a micropipette at $r = 0$) is given by:

$$C(r, t) = \frac{Q\lambda^2}{4\pi D\alpha r}\mathrm{erfc}\left(\frac{r\lambda}{2\sqrt{Dt}}\right) \tag{A2}$$

Where $C(r,t)$ gives the concentration in mol cm^{-3} of the ejected ions as a function of radial distance r in cm and time t in seconds; erfc is the complementary error function. The equation takes into consideration the tortuosity and volume fraction of the diffusion medium, but does not take into account possible contributions from enzymatic breakdown, glial uptake and any barriers resulting from tissue injury caused by the micropipette (Lalley, 1999). Nonetheless, it provides a useful upper estimate of concentration gradients and has in fact been shown to closely match experimental results in many areas of the brain (reviewed in Nicholson & Sykova, 1998). Finally, note that the concentration in mol cm^3 can be expressed in molar concentration (i.e. mol l^{-1}) by using the scale factor 1000 cm^3 l^{-1}.

Appendix 2. Propagation model

The experimental latency values we measured are due to the sum of conduction time, synaptic transmission time and synaptic integration time (time to reach firing threshold). We can write this as $L_{exp} = L_{cv} + L_{syn}$, where L_{exp} is the experimentally measured latency, L_{cv} is the latency due to axonal conduction time and L_{syn} the sum of synaptic transmission and integration times. Noting that $L_{cv} = (d - d_0)/v_c$, where d is distance, d_0 is the radius of the locus of initiation and v_c is the conduction velocity, we can write:

$$L_{\mathrm{exp}} = \frac{(d - d_0)}{v_c} + L_{syn}, \quad \text{for } d > d_0.$$

Solving for distance, we obtain:

$$d = (L_{\mathrm{exp}} - L_{\mathrm{syn}})v_c + d_0.$$

Making the assumption that L_{syn} is approximately constant, we can write:

$$d = L_{\mathrm{exp}}v_c + (d_0 - L_{\mathrm{syn}}v_c) \tag{A3}$$

The last two terms being constants, the equation can be written as a simple linear relation $d = L_{exp}v_c + k$, where $k = (d_0 - L_{syn}v_c)$. This model explains the experimentally observed y-intercept of the distance *vs.* latency graphs.

References

Ajmone-Marsan C (1969). Acute effects of topical epileptogenic agents. In *Basic Mechanisms of the Epilepsies*, ed. Jasper H, Ward AA & Pope A, pp. 299–319. Little, Brown and Company, Boston.

Buchwald JS & Grover FS (1970). Amplitudes of background fast activity characteristic of specific brain sites. *J Neurophysiol* **33**, 148–159.

Buchwald JS, Halas ES & Schramm S (1965). Comparison of multiple-unit and electro-encephalogram activity recorded from the same brain sites during behavioural conditioning. *Nature* **205**, 1012–1014.

Capaday C (2004). The integrated nature of motor cortical function. *Neuroscientist* **10**, 207–220.

Capaday C & Rasmusson DD (2003). Expansion of receptive fields in motor cortex by local blockade of GABA(A) receptors. *Experimental Brain Research* **153**, 118–122.

Capaday C, Devanne H, Bertrand L & Lavoie BA (1998). Intracortical connections between motor cortical zones controlling antagonistic muscles in the cat: a combined anatomical and physiological study. *Exp Brain Res* **120**, 223–232.

Capaday C, Ethier C, Brizzi L & Weber DJ (2006). Microelectrode array recordings of spatial activity spread in cat motor cortex. *2006 Abstract Viewer/Itinerary Planner*, Programme No. 657.4. Society for Neuroscience, Washington, DC.

Capaday C, Ethier C, Brizzi L, Sik A, van Vreeswijk C & Gingras D (2009). On the nature of the intrinsic connectivity of the cat motor cortex: evidence for a recurrent neural network topology. *J Neurophysiol* **102**, 2131–2141.

Chagnac-Amitai Y & Connors BW (1989). Horizontal spread of synchronized activity in neocortex and its control by GABA-mediated inhibition. *J Neurophysiol* **61**, 747–758.

Cheney PD & Fetz EE (1980). Functional classes of primate corticomotoneuronal cells and their relation to active force. *Journal of Neurophysiology* **44**, 773–791.

Cooke DF & Graziano MS (2004). Super-flinchers and nerves of steel: defensive movements altered by chemical manipulation of a cortical motor area. *Neuron* **43**, 585–593.

d'Avella A, Portone A, Fernandez L & Lacquaniti F (2006). Control of fast-reaching movements by muscle synergy combinations. *J Neurosci* **26**, 7791–7810.

Dayan P & Abbott LF (2001). *Theoretical neuroscience*. The MIT Press.

Donoghue JP, Leibovic S & Sanes JN (1992). Organization of the forelimb area in squirrel monkey motor cortex: representation of digit, wrist, and elbow muscles. *Experimental Brain Research* **89**, 1–19.

Ethier C, Brizzi L, Darling WG & Capaday C (2006). Linear summation of cat motor cortex outputs. *J Neurosci* **26**, 5574–5581.

Fox K, Wright N, Wallace H & Glazewski S (2003). The origin of cortical surround receptive fields studied in the barrel cortex. *J Neurosci* **23**, 8380–8391.

Golomb D & Ermentrout GB (1999). Continuous and lurching traveling pulses in neuronal networks with delay and spatially decaying connectivity. *Proc Natl Acad Sci U S A* **96**, 13480–13485.

Graziano MS, Taylor CS, Moore T & Cooke DF (2002). The cortical control of movement revisited. *Neuron* **36**, 349–362.

Grinvald A, Lieke EE, Frostig RD & Hildesheim R (1994). Cortical point-spread function and long-range lateral interactions revealed by real-time optical imaging of macaque monkey primary visual cortex. *J Neurosci* **14**, 2545–2568.

Haider B, Duque A, Hasenstaub AR & McCormick DA (2006). Neocortical network activity in vivo is generated through a dynamic balance of excitation and inhibition. *J Neurosci* **26**, 4535–4545.

Lalley PM (1999). Microiontophoresis and pressure ejection. In *Modern Techniques in Neuroscience Research*, ed. Windhorst U & Johansson H. Springer-Verlag, Berlin Heidelberg.

Lamarre Y, Bioulac B & Jacks B (1978). Activity of pre-entral neurones in conscious monkeys: effects of deafferentation and cerebellar ablation. *Journal of Physiology (Paris)* **74**, 253–264.

Legatt AD, Arezzo J & Vaughan HG Jr (1980). Averaged multiple unit activity as an estimate of phasic changes in local neuronal activity: effects of volume-conducted potentials. *J Neurosci Methods* **2**, 203–217.

Logothetis NK (2002). The neural basis of the blood-oxygen-level-dependent functional magnetic resonance imaging signal. *Philos Trans R Soc Lond B Biol Sci* **357**, 1003–1037.

Nicholson C & Phillips JM (1981). Ion diffusion modified by tortuosity and volume fraction in the extracellular microenvironment of the rat cerebellum. *J Physiol* **321**, 225–257.

Nicholson C & Sykova E (1998). Extracellular space structure revealed by diffusion analysis. *Trends Neurosci* **21**, 207–215.

Okun M & Lampl I (2008). Instantaneous correlation of excitation and inhibition during ongoing and sensory-evoked activities. *Nat Neurosci* **11**, 535–537.

Prince DA & Wilder BJ (1967). Control mechanisms in cortical epileptogenic foci. 'Surround' inhibition. *Arch Neurol* **16**, 194–202.

Sanes JN & Schieber MH (2001). Orderly somatotopy in primary motor cortex: does it exist? *Neuroimage* **13**, 968–974.

Schneider C, Zytnicki D & Capaday C (2001). Quantitative evidence for multiple widespread representations of individual muscles in the cat motor cortex. *Neurosci Lett* **310**, 183–187.

Schneider C, Devanne H, Lavoie BA & Capaday C (2002). Neural mechanisms involved in the functional linking of motor cortical points. *Exp Brain Res* **146**, 86–94.

Seidemann E, Arieli A, Grinvald A & Slovin H (2002). Dynamics of depolarization and hyperpolarization in the frontal cortex and saccade goal. *Science* **295**, 862–865.

Setlow R & Pollard E (1962). *Molecular biophysics*. Addison-Wesley, Reading, Mass.

Seutin V & Johnson SW (1999). Recent advances in the pharmacology of quaternary salts of bicuculline. *Trends Pharmacol Sci* **20**, 268–270.

Stafstrom CE, Schwindt PC & Crill WE (1984). Repetitive firing in layer V neurons from cat neocortex in vitro. *J Neurophysiol* **52**, 264–277.

Stark E & Abeles M (2007). Predicting movement from multiunit activity. *J Neurosci* **27**, 8387–8394.

Tolias AS, Sultan F, Augath M, Oeltermann A, Tehovnik EJ, Schiller PH & Logothetis NK (2005). Mapping cortical activity elicited with electrical microstimulation using FMRI in the macaque. *Neuron* **48**, 901–911.

Tremere L, Hicks TP & Rasmusson DD (2001). Expansion of receptive fields in raccoon somatosensory cortex in vivo by $GABA_A$ receptor antagonism: implications for cortical reorganization. *Exp Brain Res* **136**, 447–455.

Weiler N, Wood L, Yu J, Solla SA & Shepherd GM (2008). Top-down laminar organization of the excitatory network in motor cortex. *Nat Neurosci* **11**, 360–366.

White EL (1989). *Cortical circuits*. Birkhauser, Basel.

Author contributions

C.C. conceived the experiments, which were done by C.C., C.E. and in part by D.W. The data was analyzed by C.C. along with C.V.V., with contributions from C.E. and D.W. J.F.B. contributed to estimations of diffusion times and distances. C.C. wrote the ms. and C.V.V. contributed major editings. All authors contributed to editing the ms. The experiments were done in C.C.'s 'Brain and Movement Laboratory.'

Acknowledgements

This work was funded by a grant to C.C. from Natural Sciences and Engineering Research council of Canada and in part by one from the Canadian Institutes for Health Research (CIHR). The dedicated assistance of Ms France Roy in these experiments is gratefully acknowledged. Mr Robert Nash was involved in developing the recording arrays containing a laser etched hole and has given us invaluable and continued technical assistance with the Cerebus-128 recording system. We also thank Dr Mel Goldfinger for his comments and suggestions on a draft of the manuscript.